

Microbial associations and spatial proximity predict North American moose (*Alces alces*) gastrointestinal community composition

Nicholas M. Fountain-Jones^{*1}, Nicholas J. Clark², Amy C. Kinsley^{1,4}, Michelle Carstensen³, James Forester⁵, Timothy J. Johnson⁴, Elizabeth Miller¹, Seth Moore⁶, Tiffany M. Wolf¹ & Meggan E. Craft¹.

¹Department of Veterinary Population Medicine, University of Minnesota, St Paul, Minnesota 55108.

²UQ Spatial Epidemiology Laboratory, School of Veterinary Science, the University of Queensland, Gatton 4343, Queensland, Australia

³Minnesota Department of Natural Resources, Wildlife Health Program, 5463 West Broadway, Forest Lake, Minnesota, 55025, USA

⁴Department of Veterinary and Biomedical Sciences, University of Minnesota, St Paul, Minnesota 55108.

⁵Department of Fisheries, Wildlife and Conservation Biology, University of Minnesota, St Paul, Minnesota 55408, USA.

⁶Department of Biology and Environment, Grand Portage Band of Chippewa, Grand Portage, MN 55605

* Department of Veterinary Population Medicine, University of Minnesota, 1365 Gortner Avenue, St Paul, Minnesota 55108. nfj@umn.edu

Abstract

1. Microbial communities are increasingly recognised as crucial for animal health.

However, our understanding of how microbial communities are structured across wildlife populations is poor. Mechanisms such as interspecific associations are important in structuring free-living communities, but we still lack an understanding of how important interspecific associations are in structuring gut microbial communities in comparison to other factors such as host characteristics or spatial proximity of hosts.

2. Here we ask how gut microbial communities are structured in a population of North American moose (*Alces alces*). We identify key microbial interspecific associations within the moose gut and quantify how important they are relative to key host characteristics, such as body condition, for predicting microbial community composition.
3. We sampled gut microbial communities from 55 moose in a population experiencing decline due to a myriad of factors, including pathogens and malnutrition. We examined microbial community dynamics in this population utilizing novel graphical network models that can explicitly incorporate spatial information.\
4. We found that interspecific associations were the most important mechanism structuring gut microbial communities in moose and detected both positive and negative associations. Models only accounting for associations between microbes had higher predictive value compared to models including moose sex, evidence of previous pathogen exposure, or body condition. Adding spatial information on moose location further

strengthened our model and allowed us to predict microbe occurrences with ~90% accuracy.

5. Collectively, our results suggest that microbial interspecific associations coupled with host spatial proximity are vital in shaping infra communities in a large herbivore. In this case, previous pathogen exposure and moose body condition were not as important in predicting gut microbial community composition. The approach applied here can be used to quantify interspecific associations and gain a more nuanced understanding of the spatial and host factors shaping microbial communities in non-model hosts.

Key words: Biotic interactions, Body condition, Co-occurrence networks, Markov random fields, Microbiome, Pathogens, Spatial analysis

1 **Introduction**

2

3 The relative roles of interspecific associations versus the environment in shaping
4 communities are intensely debated (e.g., Chase & Myers, 2011; Vellend et al., 2014). In
5 particular, detecting negative (e.g., potential competition) or positive (e.g., potential
6 facilitation) associations between organisms remains a fundamental challenge of community
7 ecology (e.g., Barner, Coblenz, Hacker, & Menge, 2018; Dormann et al., 2018; Harris, 2016;
8 Ovaskainen et al., 2017). Despite the challenges of detecting associations between co-
9 occurring species, associations between species are thought to be essential for structuring
10 free-living communities (e.g., de Araújo, Marcondes-Machado, & Costa, 2014). For example,
11 associations between forest animal communities were more important in structuring
12 communities than habitat attributes such as vegetation (Le Borgne et al., 2018). In contrast,
13 the roles that interspecific associations play in governing the assembly of microbial systems
14 (*microbial interspecific associations*) are less understood (Ganz et al., 2017; Herren &
15 McMahon, 2018; Zelezniak et al., 2015), particularly for within-host microbial communities.
16 Even when microbial interspecific associations are quantified in infra-communities, the
17 relative importance of microbe dispersal (Evans, Martiny, & Allison, 2017; Zhou & Ning,
18 2017) and host characteristics in shaping microbial infra-communities is rarely assessed
19 (Clark, Wells, & Lindberg, 2018b). The quantification of interspecific associations of gut
20 microbes is rare in wildlife populations but, given the significant ecological insights derived
21 from studies of human gut microbial communities (e.g., Faust et al., 2012), is an important
22 knowledge gap to fill.

23

24 While our understanding of how microbial communities are structured is poor, it remains a
25 key goal in microbial ecology, particularly given microbial community relevance to animal

26 health. Host characteristics such as sex, body condition, and the presence or absence of
27 pathogens are recognised as important for shaping microbial infra-communities (Britton &
28 Young, 2014; Cheng et al., 2015; Ganz et al., 2017; Hooper, Littman, & Macpherson, 2012;
29 Jani & Briggs, 2014, 2018; McKenney et al., 2015; Mshelia et al., 2018; Näpflin & Schmid-
30 Hempel, 2018). For example, horses in poor body condition have greater microbial diversity
31 and a different suite of microbial species present compared to horses in good body condition
32 (Mshelia et al., 2018). High loads of the pathogen *Batrachochytrium dendrobatidis* can not
33 only increase amphibian skin microbial diversity but also alter microbial composition (Jani &
34 Briggs, 2014, 2018). However, the relative importance of host characteristics compared to
35 other ecological processes, such as interspecific associations, in structuring microbial infra-
36 communities is poorly understood.

37

38 Understanding how microbial infra-communities are shaped, however, is technically
39 challenging, in part due to the complexity of untangling complex ecological processes in
40 often species-rich but poorly characterized communities (Zhou & Ning, 2017). Graphical
41 network models such as conditional random fields (CRF) offer exciting opportunities to
42 address this challenge by estimating associations between organisms in a community (Clark,
43 Wells, & Lindberg, 2018b). In effect, these models can untangle relative influences of
44 microbial interspecific associations and host characteristics in predicting community
45 compositions. Crucially, inferences gleaned from CRFs can be integrated with phylogenetic
46 or functional data to provide new insights into mechanisms underlying microbial community
47 assembly. For example, associations between microbes may be non-random in that
48 phylogenetically or functionally similar species may co-occur more frequently (e.g., Bauer &
49 Thiele, 2018). However, non-random associations detected in the human gut have been found
50 to be often negative and between phylogenetically or functionally distinct bacterial species,

51 indicating that competition is likely an important driver of structure in this community (Faust
52 et al., 2012). Overlaying information such as this on graphical models has the potential to
53 highlight the broader mechanisms shaping microbial infra-communities.

54

55 Here we use a CRF approach to investigate microbial community composition in a wild
56 moose (*Alces alces*) population in Minnesota. Over the last two decades, moose in
57 Minnesota, which exist on the southern edge of their species range, have experienced
58 significant population decreases (Delgiudice, 2018; Lenarz, 2009). The most dramatic decline
59 has been reported for moose in northwest Minnesota, where the population declined from
60 4,000 animals in the 1980s to less than 100 by the mid-2000's due to a combination of
61 pathogens and malnutrition (Murray et al., 2006). Recently, moose in northeast Minnesota
62 have experienced a 55% population decline, driven largely by parasitic infections in adults
63 and wolf predation in calves (Carstensen et al., 2018; Severud, 2017; Wünschmann et al.,
64 2015). Moose gut microbial communities are known to vary with sex and age (Ishaq,
65 Sundset, Crouse, & Wright, 2015; Ishaq & Wright, 2012), but to what extent these host
66 characteristics, as well as pathogens and malnutrition, shape moose gut microbial
67 communities is unknown. Other ecological processes such interspecific associations, even
68 though rarely quantified in wild populations, are also likely to play a role in shaping the
69 moose gut microbial community as they do for other ruminants (Henderson et al., 2015).
70 Furthermore, animals within close proximity to each other may have similar gut microbial
71 communities due to similarities in diet and/or increased possibilities for microbial dispersal
72 between individuals; both factors known to be important in gut microbial community
73 assembly in many host species (Henderson et al., 2015; Moeller et al., 2017).

74

75 Here we apply a novel CRF approach that can quantify the relative importance of host
76 characteristics (including moose sex, body condition, pathogen exposure, and pregnancy
77 status) and microbial interspecific associations in shaping moose gut communities whilst
78 accounting for underlying spatial autocorrelation in microbial occurrences. Accounting for
79 spatial autocorrelation not only reduces false detection of interspecific associations that may
80 arise due to dispersal limitation or diet but quantifies how important these processes could be
81 in shaping microbial distributions. Specifically, we address the following questions:

- 82 1. Do CRF model combinations including host characteristics and spatial proximity
83 outperform models reflecting just associations between microbes in explaining
84 microbial communities?
- 85 2. After controlling for host characteristics and spatial patterns are there any remaining
86 non-random negative or positive associations between microbes?
- 87 3. If there are non-random associations, are they between microbes that are functionally
88 or phylogenetically similar?

89 We hypothesized that host characteristics would be the dominant processes shaping the
90 moose gut microbial community, and that spatial proximity between hosts and interspecific
91 associations would also partially explain gut microbial co-occurrence.

92 **Materials and Methods**

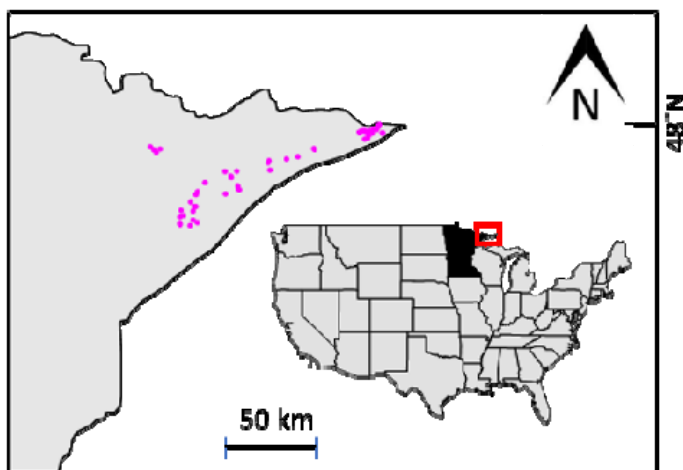
93

94 **Sample collection and sequencing**

95

96 Faecal samples were collected from 55 wild moose that were part of companion studies of
97 survival and cause-specific mortality led by the Minnesota Department of Natural Resources,
98 Grand Portage Band of Lake Superior Chippewa, and Voyageur's National Park across north-
99 eastern Minnesota (Fig. 1), placed on ice until transportation to the laboratory, and stored at -
100 20°C prior to processing. This included moose that were live-captured (n = 52, 2011-2015)

101 and sick (n = 3, 2009-2010). Details of the capture and handling of these moose can be found
102 in Butler et al. (2012) and Carstensen et al. (2018). The metadata provided from these moose
103 included date and location of capture, pregnancy status, sex, age, body condition, and
104 serological exposure to *Borrelia burgdorferi*, West Nile Virus, and leptospira (6 serovars
105 including *L. bratislava*, *L. canicola*, *L. grippityphosa*, *L. hardjo*, *L. icterohemorrhagica* and
106 *L. pomona*). In total, we had serological data for 49 moose (33 females and 16 males) with
107 the remaining 6 individuals removed from the CRF analysis (but retained for the descriptive
108 analysis). See Butler et al. (2012) for serological test details. Of the live-captured moose, 21
109 were observed to be underweight (thin/very thin), and 31 were considered of normal body
110 condition at winter capture (Jan-Feb). All samples apart from one were collected in winter
111 between 2011- 2015; the other sample was collected in 2003. Microbial DNA was extracted
112 from the faecal samples using the PowerSoil DNA Isolation kit (Qiagen), in accordance with
113 the manufacturer's protocol. The V4 hypervariable region of the bacterial 16S rRNA gene
114 was amplified using the barcoding primers 515F and 806R. Amplicons were sequenced on
115 the Illumina MiSeq platform following the method outlined by Gohl et al., (2016).



116
117 **Figure 1:** Locations (pink dots) of moose faecal samples in northeastern Minnesota, USA.
118 The red box shows the location of the study in Minnesota.

119

120 **Bioinformatics pipeline**

121

122 Raw sequencing reads were processed using the University of Minnesota's metagenomics-

123 pipeline (complete description of the pipeline can be found at

124 <https://bitbucket.org/jgarbe/gopher-pipelines/overview>), which implements the QIIME

125 version 1.9.1 analysis software (Caporaso et al., 2010). Briefly, sequencing adaptors were

126 trimmed using Trimmomatic (Bolger, Lohse, & Usadel, 2014) and read pairs were assembled

127 and primer sequences removed using PANDAseq (Masella, Bartram, Truszkowski, Brown, &

128 Neufeld, 2012). Reads without primers, unpaired reads, and assembled reads that were

129 outside the expected rRNA gene V4 region length were discarded. Chimeras were detected

130 and removed with QIIME's identify_chimeric_seqs.py function with the usearch61 algorithm

131 (Edgar, 2010). Open-reference OTU (operational taxonomic unit) picking was conducted

132 using QIIME's pick_open_reference_otus.py with a minimum sequence identity threshold of

133 97%. Representative OTU sequences were aligned against the Greengenes 18.8 core set

134 (DeSantis et al., 2006b) using UCLUST (Edgar, 2010) with QIIME default parameters.

135 Singleton OTUs and those that did not align with PyNAST (Caporaso et al., 2010) were

136 removed from the analysis. To control for differences in sequencing depth between samples,

137 read counts were rarefied to the lowest number of reads (101,131) per sample.

138

139 To test for co-occurrence patterns between gut microbes, we filtered out OTUs with $\leq 10\%$

140 abundance (i.e., only keeping OTUs that occurred in at least 10% of samples) and converted

141 the OTU table into a presence-absence matrix. OTUs that were found $\geq 75\%$ of samples were

142 also filtered from the analysis. Our purpose for removing rare and common OTUs was to

143 ensure that adequate inferences could be made about the occurrence probability of each OTU

144 (Ovaskainen, Abrego, Halme, & Dunson, 2016). This would be difficult / impossible to do if

145 the target OTU shows little variability across sampled environmental gradients by being

146 either too rare or too common. We transformed the presence-absence matrix into a Jaccard

147 similarity matrix and used non-metric multidimensional scaling (NMDS) to select OTUs that
148 were driving compositional change across the moose samples and therefore likely to differ
149 with moose characteristics such as body condition (Pearson correlation coefficient > 0.45). In
150 total, 42 OTUs remained after this filtering process. NMDS was performed using functions in
151 the R package *vegan* (Oksanen et al., 2013).

152

153 To reduce the dimensions of the serological exposure data for subsequent analysis, we
154 converted test results into a binary matrix (0 if the individual tested negative and 1 if
155 positive), transformed the binary matrix into a Jaccard similarity matrix, and then performed
156 principal coordinate analysis (PCoA) using the R package *vegan* (Oksanen et al., 2013). The
157 first three PCoA axes represented 85% of the variation in exposure across individuals and
158 eigenvalues from these axes were used as covariates in the CRF analysis below (now called
159 *pathogen exposure PCoA axes*).

160

161 **Conditional random fields**

162

163 *Identifying OTU co-occurrence patterns using conditional random fields*

164 The framework we used to investigate OTU co-occurrence probabilities while accounting for
165 potential influences of covariates is described in detail by Clark et al. (2018a) and references
166 therein. Briefly, the log-odds of observing OTU j given covariate x and the presence-absence
167 of OTU k is modelled using:

$$\log \left(\frac{P(y_j = 1 | y_{\setminus j}, x)}{1 - P(y_j = 1 | y_{\setminus j}, x)} \right) = \alpha_{j0} + \beta_j^T x + \sum_{k: k \neq j} (\alpha_{jk0} + \beta_{jk}^T x) y_k \quad (1)$$

168 where y_j is a vector of binary observations for OTU j (1 if the OTU was present, 0 if absent),
169 $y_{\setminus j}$ represents vectors of binary observations for all other OTUs apart from j , α_{j0} is the OTU-
170 level intercept, and β_j^T is the coefficient for the effect of covariate x on OTU j 's occurrence

171 probability. Interaction parameters are represented by α_{jko} and β_{jkx}^T (defined below).
172 Parameterization of the likelihood is estimated using logistic regression, where regression
173 coefficients represent the effects of predictors on the OTU's conditional log-odds. Cross-
174 multiplying all combinations of co-occurring OTUs and external covariates allows direct
175 comparison of the relative influences interspecific associations) and host effects on an OTU's
176 occurrence probability. For each OTU-specific regression, sparsity is added to the model
177 using L1 (e.g., least absolute shrinkage and selection operator [LASSO]) regularisation to
178 force regression coefficients toward zero if they have minimal effects. Ten-fold cross-
179 validation was implemented to choose the penalty that minimised cross-validated error, as
180 this is considered an appropriate loss function in binomial classification studies. Following
181 LASSO variable selection, coefficients representing conditional dependence of two OTUs
182 and coefficients representing effects of covariates on this dependence were symmetrized by
183 taking the mean of the corresponding estimates so that $\alpha_{jko} = \alpha_{kjo}$ and $\beta_{jkx}^T = \beta_{kx}^T$. This means
184 we can approximate parameters from a unified graphical network, after maximizing the
185 conditional log-likelihood for each OTU (Lee & Hastie, 2015). Following unification,
186 inference is straightforward. If $\alpha_{jko} = 0$, we can infer that the occurrence probabilities of
187 OTUs j and k are conditionally independent, after accounting for covariates and other OTUs.
188 If $\alpha_{jko} \neq 0$ but $\beta_{jkx}^T = 0$, the occurrence probabilities are still considered conditionally
189 dependent, but the strength of this dependence is not expected to co-vary with covariate x .

190

191 *MRF and CRF model selection*

192 We estimated four graphical model formulations of increasing complexity to identify a best-
193 fitting model for our OTU presence-absence dataset. In the first, we built a Markov random
194 fields (MRF) graph that did not include any spatial data or host characteristics and used only
195 the binary occurrences of the 42 OTUs as predictors (hereafter the *MRF model*). In the

196 second model, the GPS coordinates for each observation (latitude and longitude, in decimal
197 degrees) were used to construct penalised Gaussian process regression splines with 100
198 degrees of freedom (Kammann & Wand, 2003; Wood, 2003) (hereafter the *spatial MRF*
199 *model*). Including the spatial splines in each OTU's linear predictor ensured that interspecific
200 associations on occurrence probabilities were estimated only after accounting for possible
201 spatial autocorrelation. For the third model, we built a CRF including moose characteristics
202 covariates (moose sex, body condition, pregnancy status and the pathogen exposure PCoA
203 axes) as well as longitude and latitude (hereafter the *non-spatial CRF model*). All covariates
204 were included as scaled continuous variables with the exceptions of sex and pregnancy status,
205 which were both included as categorical variables. For the final model, we built a CRF as
206 above, but we replaced the latitude and longitude variables with spatial splines (hereafter the
207 *spatial CRF model*).

208

209 We assessed the fit of each of the above candidate models to the observed data by calculating
210 the proportion of observations that each model successfully classified. This was done using
211 ten-fold cross-validation. The best-fitting model was then fit to 100 bootstrapped versions of
212 the observed data (randomly shuffling observations in each bootstrap iteration) to capture
213 uncertainty in model parameters. All CRF model fitting was performed using functions in the
214 *MRFcov* R package (Clark, Wells, & Lindberg, 2018a). From the OTU co-occurrence data,
215 we constructed an adjacency matrix and plotted association networks using *iGraph* R
216 package (Csárdi & Nepusz, 2006). See Appendix S1 for R code detailing data preparation,
217 analytical routine and model specification.

218

219 **OTU functional predictions**

220

221 We predicted the molecular functions of OTUs using PICRUSt's precalculated functional
222 prediction table, where the rows were KEGG orthologs (KOs) and the columns were OTUs
223 based on Greengenes identification numbers (DeSantis et al., 2006a; Kanehisa, Sato,
224 Kawashima, Furumichi, & Tanabe, 2016; Langille et al., 2013). This KO table was converted
225 into a presence-absence matrix (i.e., whether a particular functional ortholog is associated
226 with that OTU) and calculated the pairwise functional similarity using the Jaccard index. We
227 applied NMDS to view the broad functional relationships between OTUs and define
228 functional groups (FGs).

229 **Results**

230

231 We found that Firmicutes, followed by Bacteroidetes, were the dominant phyla in all our
232 moose gut communities making up over 75% of the reads detected (Fig. S1). The ratio of
233 these groups across samples was relatively consistent with only one individual having a
234 proportion < 50% of Firmicutes present (Fig. S2). Functionally the OTUs could be grouped
235 into two FGs (Fig. S3).

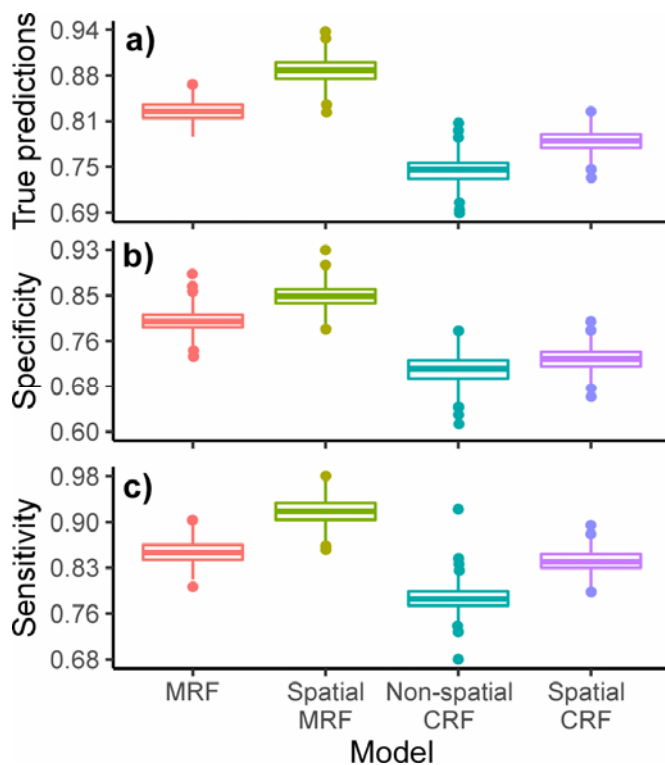
236

237 **Model fit**

238

239 The MRF model, which only quantified associations between microbes, could more
240 accurately predict OTU occurrence compared to either the spatial CRF or non-spatial CRF
241 models (both of which included host characteristics; Fig. 2a). Including spatial regression
242 splines did improve the fit of the CRF model, with this model accurately predicting 78% of
243 observations compared to 74% of for the non-spatial CRF (Fig. 2a). In contrast, the MRF
244 could accurately predict 83% of presence-absence observations on average (Fig. 2a). This
245 result was not due to one model being better able to predict occurrence over absence, as the
246 MRF had much higher specificity and sensitivity than either of the CRF models (Fig. 2b/c).
247 However, we still found evidence of spatial clustering in microbial occurrence probabilities,

248 as MRF performance improved further when we included spatial splines in the model (Fig.
249 2a). Adding spatial data to this model enabled us to correctly predict ~90% of OTU
250 occurrences in the moose gut microbial community. This not only suggests that microbes in
251 our dataset were more likely to show similar occurrences in moose that were sampled nearby
252 to one another, but that false associations between microbes could be inferred by models that
253 do not account for spatial proximity.



254
255 **Figure 2:** Box and whisker plots showing the predictive performance of the Markov random
256 field model (MRF – without model covariates), spatial MRF model, non-spatial conditional
257 random field model (CRF - with model covariates) and spatial CRF as defined by (a) true
258 prediction performance, b) specificity, and c) sensitivity. Predictions were assessed by fitting
259 models to a random fold containing 90% of the data (training data) and predicting
260 observations for the remaining 10% (test data). This process was repeated 100 times to
261 capture uncertainty in performance. Specificity is the ability of the model to correctly identify
262 individual moose without the specified OTU (proportion of observed negatives that were

263 predicted to be negative), while sensitivity is the ability to correctly identify individuals with
264 the specified OTU (proportion of observed positives that were predicted to be positive). Box
265 hinges show the interquartile range (25% and 75% quantiles), lines within boxes indicate the
266 median (50% quantile), whiskers show 10% and 90% quantiles and dots show values outside
267 these quantiles.

268

269 **Microbial associations**

270

271 The co-occurrence network revealed that both positive and negative associations occurred
272 across taxonomic and functional groups with no clear phylogenetic pattern (i.e., OTUs from
273 the same phyla/class or function were not preferentially negatively or positively associated
274 with each other, Fig. 3). On average, we found that positive associations between OTUs were
275 more common than negative associations (4 vs 2, Table 1). Firmicutes was the best-
276 represented phyla in our moose faecal samples (Fig. S1), and this phylum also had the highest
277 number of OTU associations. Strikingly, even though Bacteroidetes was the second most
278 dominant phyla, we did not detect any associations involving OTUs from this taxa. In
279 contrast, OTUs from Tenericutes were rare (3% of sequences, Fig. S1), but overall, they had
280 on average 1 more positive association partner than other phyla (4 vs 3), whereas
281 Cyanobacteria OTUs had more negative association partners than other phyla (3 vs 2, Table
282 1). FGs showed similar differences, with FG1 (which was dominated by the Tenericutes; Fig.
283 S3) having more positive associations compared to FG2 (4 vs 3 on average). The opposite
284 was true for negative associations, with FG2 having more associations on average than FG1
285 (1 vs 2). Overall, two previously uncharacterized OTUs (identified by the 'NewReference'
286 label) from class Mollicutes (Tenericutes) and class Clostridia (Firmicutes) had the highest
287 number of associations overall (8, Table 1). Two OTUs from class Clostridia had the highest
288 numbers of negative associations (5 & 6 respectively, Table 1).

289 **Table 1:** Summary of associations detected in the MRF analysis.

OTU identity	Avg.oc	Pos	Neg	Phylum Class	FG
338145	0.2043	6	4	Actinobacteria Coriobacteriia	2
NewReferenceOTU314	0.6637	2	1	Actinobacteria Coriobacteriia	N
NewReferenceOTU69	0.6832	2	1	Actinobacteria Coriobacteriia	N
NewReferenceOTU74	0.7562	3	2	Actinobacteria Coriobacteriia	N
206930	0.4799	4	4	Cyanobacteria 4C0d-2	2
NewReferenceOTU123	0.5473	6	3	Cyanobacteria 4C0d-2	N
NewReferenceOTU73	0.5461	0	2	Cyanobacteria Chloroplast	N
322906	0.9437	3	4	Firmicutes Clostridia	2
325706	0.6148	0	1	Firmicutes Clostridia	2
4317006	0.0372	5	4	Firmicutes Clostridia	2
4480841	0.5291	2	1	Firmicutes Clostridia	2
4314603	0.4536	2	1	Firmicutes Clostridia	2
4417708	0.0843	7	4	Firmicutes Clostridia	2
296918	0.7692	1	4	Firmicutes Clostridia	2
266952	0.6309	3	3	Firmicutes Clostridia	2
294064	0.5084	5	3	Firmicutes Clostridia	2
294262	0.2403	6	1	Firmicutes Clostridia	2
579159	0.2068	3	2	Firmicutes Clostridia	2
333577	0.3276	2	1	Firmicutes Clostridia	2
1038874	0.3899	2	0	Firmicutes Clostridia	2
129755	0.3879	3	0	Firmicutes Clostridia	2
738351	0.6364	1	0	Firmicutes Clostridia	2
4295783	0.3693	1	0	Firmicutes Clostridia	2
574585	0.6326	1	5	Firmicutes Clostridia	2
NewReferenceOTU108	0.0809	8	3	Firmicutes Clostridia	N
NewReferenceOTU74	0.3172	1	0	Firmicutes Clostridia	N
NewReferenceOTU76	0.2891	5	6	Firmicutes Clostridia	N
NewReferenceOTU76	0.0827	6	4	Firmicutes Clostridia	N
NewReferenceOTU157	0.0899	3	0	Firmicutes Clostridia	N
NewReferenceOTU289	0.1515	5	4	Firmicutes Clostridia	N
4396877	0.0928	5	1	Firmicutes Erysipelotrichi	2
NewReferenceOTU42	0.5286	3	4	Firmicutes Erysipelotrichi	N
339838	0.063	1	1	Tenericutes Mollicutes	1
513605	0.0299	7	1	Tenericutes Mollicutes	1
4446732	0.6627	4	2	Tenericutes Mollicutes	1
1108356	0.5123	4	2	Tenericutes Mollicutes	1
921020	0.1596	5	1	Tenericutes Mollicutes	1
NewReferenceOTU413	0.2271	5	2	Tenericutes Mollicutes	N
NewReferenceOTU493	0.2445	4	1	Tenericutes Mollicutes	N
NewReferenceOTU390	0.6923	0	0	Tenericutes Mollicutes	N
NewReferenceOTU404	0.1345	8	2	Tenericutes Mollicutes	N
NewReferenceOTU528	0.4842	4	4	Tenericutes RF3	N
Average		4	2		

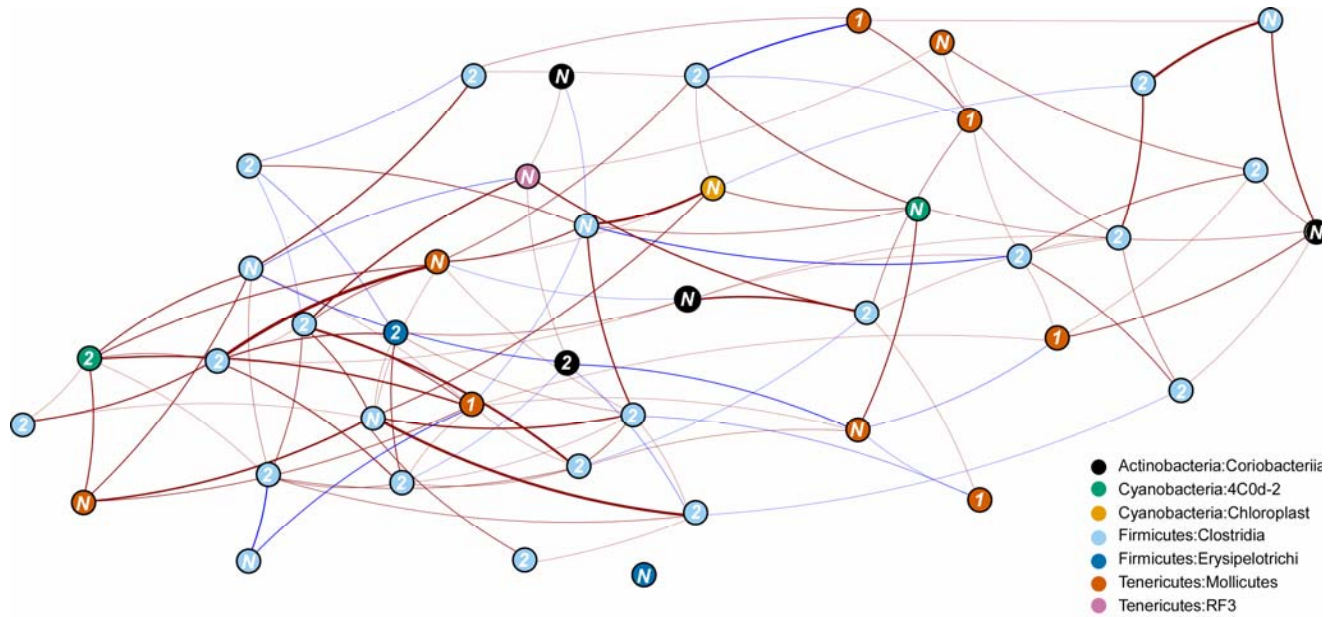
290 Avg.oc: average occurrence in our moose samples. Pos: number of positive associations.

291 Neg: number of negative associations. 'NewReference' indicates that the OTU has not been

292 previously characterised by the Greengenes database. FG: Functional group (see Figure S3).

293 N: No functional group could be determined (not previously characterized).

294



295

296

Figure 3: Moose gut microbial MRF co-occurrence network. Blue edges indicate negative

297

associations and red edges represent positive associations. Edge thickness is scaled by the

298

strength of association. Node colour indicates taxonomic group of each microbe. Numbers on

299

the node represent which broad functional group (FG) each OTU belonged to (see Fig. S3).

300

‘N’ indicates that there was no functional data for this microbe. See Fig. S4 for the OTU

301

correlation matrix with names included.

302 Discussion

303

304 Utilizing graphical network models, we show the importance of microbial interspecific

305

associations over host characteristics in shaping moose gut microbial communities at a

306

population scale. In this case, both interspecific associations and spatial proximity were

307

important for shaping microbial communities in this declining moose population. Host

308

characteristics were relatively less important in predicting the distribution of microbes. Even

309

though we did not have host genetic or specific diet data from individuals (i.e. stable isotope

310

data), we could predict microbial distributions using just interspecific associations with

311

remarkably high accuracy. Across this moose population, we detected non-random negative

312 and positive microbial associations with no clear functional or phylogenetic pattern. Our
313 study not only highlights the importance of accounting for interspecific associations when
314 trying to quantify how host characteristics shapes host infra-communities but also shows the
315 value of graphical network models in untangling community dynamics more broadly.

316

317 We found that evidence of pathogen exposure was not particularly important in predicting
318 moose gut microbial community dynamics. As the serological evidence we used in this study
319 only infers past infection by a particular pathogen rather than current infection status, perhaps
320 this is not surprising. Previous studies testing the role of pathogens shaping microbial
321 communities have used evidence of current infection (e.g., qPCR; Ganz et al., 2017;
322 McKenney et al., 2015) rather than previous exposure based on serological evidence. When
323 we sampled the moose gut microbial communities, the animal may not be experiencing the
324 infection, and this may be the reason we did not detect an effect. It is also possible that
325 herbivore gut microbial communities are more resilient to pathogen infection than other
326 trophic groups such as carnivores. Ruminant microbial communities are more dominated by
327 environmental bacteria cultivated by the host to aid digestion (Muegge et al., 2011) and may
328 be less regulated by the immune system compared to the gut microbial communities in other
329 species (Ley et al., 2008). Lower immune regulation, for example, could explain why the
330 herbivores such as the gorilla (*Gorilla gorilla*) have microbiomes remarkably resilient to
331 Simian immunodeficiency virus infection compared to omnivorous chimpanzees (*Pan*
332 *trogodytes*) or for HIV infection in humans (Moeller et al., 2015). In support of this, we find
333 that across individual moose in our study, the relative proportions of gut microbial taxa were
334 relatively consistent, despite large differences in body condition and exposure status (Fig.
335 S2). Similar ratios of the different microbial taxa in moose have also been reported in moose
336 from the east coast of North America (Ishaq & Wright, 2012) even though samples were

337 collected from moose in a different season. Further studies where current pathogen infection
338 status is known in moose and other herbivores are needed to resolve this question.

339

340 Interspecific associations, in contrast, were much better predictors of moose gut microbial
341 communities. In free-living communities, the role of interspecific associations in shaping the
342 distributions of species is increasingly recognised (e.g., Aragón, Carrascal, & Palomino,
343 2018; C. B. de Araújo et al., 2014). However, the importance of interspecific associations is
344 likely to decrease with geographic scale (Araújo & Rozenfeld, 2014). Whether this applies to
345 gut microbial communities, in contrast, is poorly studied. In our case, host effects may have
346 been detectable if we sampled a greater number of individuals across a larger portion of
347 moose home range in central North America. Nonetheless, the scale at which wildlife
348 surveillance is performed (and thus faecal samples collected for gut microbiome analysis) is
349 often similar across studies (e.g., Cheng et al., 2015). In general, understanding the role that
350 scale plays in structuring gut microbial communities, beyond the population scale, is a major
351 challenge for microbial ecology (Antwis et al., 2017; Camp, Kanther, Semova, & Rawls,
352 2009). Based on our findings, we suggest that larger geographical and/or temporal scales are
353 needed to detect possible impacts of host characteristics on the structure of gut microbial
354 communities.

355

356 Even without accounting for host traits such as host genetics that are thought to be important
357 in shaping the gut microbial communities in other herbivores (Kohl, Varner, Wilkening, &
358 Dearing, 2017), our models had high predictive performance. Our results may be due to
359 samples coming from a relatively well-mixed population, even though our moose samples
360 were taken over a large area spanning a maximum of ~150 km. Central North America
361 (including Minnesota) has the highest genetic diversity of all North American moose

362 populations (Hundertmark, Bowyer, Shields, & Schwartz, 2003), but to what extent our
363 samples come from genetically distinct populations is unknown. Future work incorporating
364 host genetics in moose may help better understand the role of host characteristics, compared
365 to microbial interspecific associations in shaping infra-communities.

366

367 Our capacity to predict the moose gut microbial community at the population scale increased
368 when we included spatial information, indicating that either stochastic events such as
369 microbial dispersal or spatial similarities in diet may be important in structuring associations
370 between gut microbes. Dispersal of microbes is thought to be passive (Nemergut et al., 2013),
371 however, these microbial species are often in high abundance and have broad distributions
372 making dispersal challenging to quantify (Evans et al., 2017; Zhou & Ning, 2017).

373 Biogeographical studies have shown that dispersal limitation is important for structuring
374 microbial communities including those of the gut (Evans et al., 2017; Hanson, Fuhrman,
375 Horner-Devine, & Martiny, 2012; Moeller et al., 2017), but rarely over a relatively small area
376 within a host population. What role moose diet explicitly played in shaping our moose gut
377 microbial communities is still an open question. Future studies linking host microbial data to
378 measures of host diet, such as stable isotope analysis (Hofman-Kamińska, Bocherens,
379 Borowik, Drucker, & Kowalczyk, 2018), will enable dispersal limitation and diet to be
380 decoupled in future models. Nonetheless, we show that including host spatial data in future
381 work is necessary for robustly quantifying microbial co-occurrence patterns.

382

383 We also found strong positive and negative associations between OTUs from different phyla
384 and divergent functional groups in the moose gut microbial community. Clostridia
385 (Firmicutes) and Mollicutes (Tenericutes) were network ‘hubs’ involved in a relatively high
386 number of positive associations in our moose population, and often with each other (Table 1).

387 Clostridia OTUs are also hubs for associations in the human gut community (Banerjee,
388 Schlaeppli, & van der Heijden, 2018; Faust et al., 2012), but the importance of Mollicutes has
389 not been, to our knowledge, reported elsewhere. Moreover, we detected no negative
390 associations between Bacteroidetes and Firmicutes even though Bacteroidetes was common
391 in our samples; this group may not play a dominant role in structuring moose gut microbial
392 communities as they do in humans (Banerjee et al., 2018; Faust et al., 2012). Whether the
393 same relationships apply in herbivore populations where Bacteroidetes is dominant, as was
394 the case in an Alaskan and Swedish moose (Ishaq & Wright, 2014; Svartström et al., 2017),
395 remains an open question. More generally, Faust et al. (2012) found an increased likelihood
396 of negative associations between OTUs that were functionally and phylogenetically
397 dissimilar (with opposite true for more related OTUs). We did not see such a pattern in our
398 co-occurrence network and why we would get such a different result in moose is unclear. The
399 Faust dataset consisted of 240 individuals from the Human Microbiome Project (Methé et al.,
400 2012), but large methodological differences make direct comparison difficult, as factors such
401 as spatial relationships between subjects were not quantified. How robust these relationships
402 are also likely to be impacted by taxonomic resolution of each network (Faust et al., 2012).
403 As we used 16S rRNA gene sequencing, we were unable to get sequence identifications to
404 species level. Further, functional profiles were based on predictions from reference genomes,
405 not direct identification of functional genes or proteins (Langille et al., 2013). Shotgun
406 metagenomic sequencing could allow for both classification sequences to species-level and
407 provide much more detailed insights into the functional patterns shaping microbial species
408 associations.

409

410 Here we have demonstrated that graphic network models can untangle how interspecific
411 interactions can shape gut microbial communities in moose. Additionally, we show that MRF

412 and CRF models can robustly construct co-occurrence networks (Clark, Wells, & Lindberg,
413 2018b) and, coupled with taxonomic and functional information, find high-resolution insights
414 into interspecific associations. Graphical network models, as with other correlation-based
415 approaches, do have limitations. Correlations identified by techniques such as MRF or CRF
416 should be treated with caution as they do not imply causation (e.g., Barner et al., 2018;
417 Dormann et al., 2018). Follow up analysis with tools such as structural equation modelling
418 (SEM) could be used to go beyond correlations to explore potential causal relationships
419 between microbes (Banerjee et al., 2018). Nonetheless, by explicitly incorporating spatial
420 data and covariates into graphical models, our method offers a step forward in characterising
421 associations between species, and we envisage this method will be broadly useful for
422 researchers working on micro- and macro-community dynamics alike. Studies analysing
423 associations between infra-community microbial species are rare in wildlife, even though
424 they can provide important insights into the ecological dynamics operating within or on the
425 host. Given the decreasing cost of microbial surveys and analytical advances such as ours,
426 studies that can disentangle microbial infra-community dynamics in wildlife species will
427 become more frequent, and this can ultimately provide a more nuanced understanding of
428 wildlife health.

429

430 **Acknowledgements**

431 This material is based upon work supported by the Cooperative State Research Service, U.S.
432 Department of Agriculture, under Project No. MINV-62-051.

433

434 **Data accessibility**

435

436 All data will be made accessible in Dryad.

437

438 **Author contribution statement.**

439

440 NFJ, MC, TW, JF, TJ, AK and MEC came up with the project design. NFJ, NC and EM

441 conducted the analysis. NC coded the spatial MRF/CRF functions. MC, TW, SM and JF

442 provided data. All authors contributed critically to the drafts and gave final approval for

443 publication.

444

445 **References**

446

447 Antwis, R. E., Griffiths, S. M., Harrison, X. A., Aranega-Bou, P., Arce, A., Bettridge, A. S.,

448 ... Sutherland, W. J. (2017). Fifty important research questions in microbial ecology.

449 *FEMS Microbiology Ecology*, 93(5). doi:10.1093/femsec/fix044

450 Aragón, P., Carrascal, L. M., & Palomino, D. (2018). Macro-spatial structure of biotic

451 interactions in the distribution of a raptor species. *Journal of Biogeography*, 45(8),

452 1859–1871. doi:10.1111/jbi.13389

453 Araújo, M. B., & Rozenfeld, A. (2014). The geographic scaling of biotic interactions.

454 *Ecography*, 37(5), 406–415. doi:10.1111/j.1600-0587.2013.00643.x

455 Banerjee, S., Schlaeppli, K., & van der Heijden, M. G. A. (2018). Keystone taxa as drivers of

456 microbiome structure and functioning. *Nature Reviews Microbiology*, 16(9), 567–576.

457 doi:10.1038/s41579-018-0024-1

458 Barner, A. K., Coblenz, K. E., Hacker, S. D., & Menge, B. A. (2018). Fundamental

459 contradictions among observational and experimental estimates of non-trophic species

460 interactions. *Ecology*, 99(3), 557–566. doi:10.1002/ecy.2133

461 Bauer, E., & Thiele, I. (2018). From network analysis to functional metabolic modeling of the

462 human gut microbiota. *MSystems*, 3(3), e00209-17. doi:10.1128/mSystems.00209-17

463 Bolger, A. M., Lohse, M., & Usadel, B. (2014). Trimmomatic: a flexible trimmer for Illumina

- 464 sequence data. *Bioinformatics*, 30(15), 2114–2120. doi:10.1093/bioinformatics/btu170
- 465 Britton, R. A., & Young, V. B. (2014). Role of the intestinal microbiota in resistance to
466 colonization by *Clostridium difficile*. *Gastroenterology*, 146(6), 1547–1553.
467 doi:10.1053/j.gastro.2014.01.059
- 468 Butler, E., Carstensen, M., Hildebrand, E., & Giudice, J. (2012). Northeast Minnesota moose
469 herd health assessment 2007–2012. In L. Cornicelli, M. Carstensen, M. Grund, M.
470 Larson, & Lawrence JS (Eds.), *Summaries of wildlife research findings 2012*. St Paul:
471 Minnesota Department of Natural Resources. Retrieved from <http://www.mndnr.gov>
- 472 Camp, J. G., Kanther, M., Semova, I., & Rawls, J. F. (2009). Patterns and scales in
473 gastrointestinal microbial ecology. *Gastroenterology*, 136(6), 1989–2002.
474 doi:10.1053/j.gastro.2009.02.075
- 475 Caporaso, J. G., Bittinger, K., Bushman, F. D., DeSantis, T. Z., Andersen, G. L., & Knight,
476 R. (2010). PyNAST: a flexible tool for aligning sequences to a template alignment.
477 *Bioinformatics*, 26(2), 266–267. doi:10.1093/bioinformatics/btp636
- 478 Caporaso, J. G., Kuczynski, J., Stombaugh, J., Bittinger, K., Bushman, F. D., Costello, E. K.,
479 ... Knight, R. (2010). QIIME allows analysis of high-throughput community sequencing
480 data. *Nature Methods*, 7(5), 335–336. doi:10.1038/nmeth.f.303
- 481 Carstensen, M., Hildebrand, E. C., Plattner, D., Dexter, M., St-Louis, V., Jennelle, C., &
482 Wright, R. G. (2018). *Determining cause specific mortality of adult moose in Northeast*
483 *Minnesota, February 2013 - July 2017*. Retrieved from
484 [https://files.dnr.state.mn.us/wildlife/research/summaries/health/2016_moose-](https://files.dnr.state.mn.us/wildlife/research/summaries/health/2016_moose-mortality.pdf)
485 [mortality.pdf](https://files.dnr.state.mn.us/wildlife/research/summaries/health/2016_moose-mortality.pdf)
- 486 Chase, J. M., & Myers, J. A. (2011). Disentangling the importance of ecological niches from
487 stochastic processes across scales. *Philosophical Transactions of the Royal Society B:*
488 *Biological Sciences*, 366(1576), 2351–2363. doi:10.1098/rstb.2011.0063

- 489 Cheng, Y., Fox, S., Pemberton, D., Hogg, C., Papenfuss, A. T., & Belov, K. (2015). The
490 Tasmanian devil microbiome—implications for conservation and management.
491 *Microbiome*, 3(1), 76. doi:10.1186/s40168-015-0143-0
- 492 Clark, N. J., Wells, K., & Lindberg, O. (2018). MRFCov: Markov Random Fields with
493 additional covariates. R package version 1.0.33. Availabe at GitHub.
494 <https://github.com/nicholasjclark/MRFCov>.
- 495 Clark, N. J., Wells, K., & Lindberg, O. (2018). Unravelling changing interspecific
496 interactions across environmental gradients using Markov random fields. *Ecology*,
497 99(6), 1277–1283. doi:10.1002/ecy.2221
- 498 Csárdi, G., & Nepusz, T. (2006). The igraph software package for complex network research.
499 *InterJournal Complex Systems*, 1695.
- 500 de Araújo, C. B., Marcondes-Machado, L. O., & Costa, G. C. (2014). The importance of
501 biotic interactions in species distribution models: a test of the Eltonian noise hypothesis
502 using parrots. *Journal of Biogeography*, 41(3), 513–523. doi:10.1111/jbi.12234
- 503 Delgiudice, G. D. (2018). *2018 Aerial Moose Survey*. Retrieved from
504 <https://files.dnr.state.mn.us/wildlife/moose/moosesurvey.pdf>
- 505 DeSantis, T. Z., Hugenholtz, P., Larsen, N., Rojas, M., Brodie, E. L., Keller, K., ...
506 Andersen, G. L. (2006a). Greengenes, a chimera-checked 16S rRNA gene database and
507 workbench compatible with ARB. *Applied and Environmental Microbiology*, 72(7),
508 5069–72. doi:10.1128/AEM.03006-05
- 509 DeSantis, T. Z., Hugenholtz, P., Larsen, N., Rojas, M., Brodie, E. L., Keller, K., ...
510 Andersen, G. L. (2006b). Greengenes, a chimera-checked 16S rRNA gene database and
511 workbench compatible with ARB. *Applied and Environmental Microbiology*, 72(7),
512 5069–5072. doi:10.1128/AEM.03006-05
- 513 Dormann, C. F., Bobrowski, M., Dehling, D. M., Harris, D. J., Hartig, F., Lischke, H., ...

- 514 Kraan, C. (2018). Biotic interactions in species distribution modelling: 10 questions to
515 guide interpretation and avoid false conclusions. *Global Ecology and Biogeography*.
516 doi:10.1111/geb.12759
- 517 Edgar, R. C. (2010). Search and clustering orders of magnitude faster than BLAST.
518 *Bioinformatics*, 26(19), 2460–2461. doi:10.1093/bioinformatics/btq461
- 519 Evans, S., Martiny, J. B. H., & Allison, S. D. (2017). Effects of dispersal and selection on
520 stochastic assembly in microbial communities. *The ISME Journal*, 11(1), 176–185.
521 doi:10.1038/ismej.2016.96
- 522 Faust, K., Sathirapongsasuti, J. F., Izard, J., Segata, N., Gevers, D., Raes, J., & Huttenhower,
523 C. (2012). Microbial co-occurrence relationships in the human microbiome. *PLoS*
524 *Computational Biology*, 8(7), e1002606. doi:10.1371/journal.pcbi.1002606
- 525 Ganz, H. H., Doroud, L., Firl, A. J., Hird, S. M., Eisen, J. A., & Boyce, W. M. (2017).
526 Community-level differences in the microbiome of healthy wild mallards and those
527 infected by Influenza A viruses. *mSystems*, 2(1), e00188-16.
528 doi:10.1128/mSystems.00188-16
- 529 Gohl, D. M., Vangay, P., Garbe, J., MacLean, A., Hauge, A., Becker, A., ... Beckman, K. B.
530 (2016). Systematic improvement of amplicon marker gene methods for increased
531 accuracy in microbiome studies. *Nature Biotechnology*, 34(9), 942–949.
532 doi:10.1038/nbt.3601
- 533 Hanson, C. A., Fuhrman, J. A., Horner-Devine, M. C., & Martiny, J. B. H. (2012). Beyond
534 biogeographic patterns: processes shaping the microbial landscape. *Nature Reviews*
535 *Microbiology*, 10(7), 497–506. doi:10.1038/nrmicro2795
- 536 Harris, D. J. (2016). Inferring species interactions from co-occurrence data with Markov
537 networks. *Ecology*, 97(12), 3308–3314. doi:10.1002/ecy.1605
- 538 Henderson, G., Cox, F., Ganesh, S., Jonker, A., Young, W., Global Rumen Census

- 539 Collaborators, G. R. C., & Janssen, P. H. (2015). Rumen microbial community
540 composition varies with diet and host, but a core microbiome is found across a wide
541 geographical range. *Scientific Reports*, 5, 14567. doi:10.1038/srep14567
- 542 Herren, C. M., & McMahon, K. D. (2018). Keystone taxa predict compositional change in
543 microbial communities. *Environmental Microbiology*, 20(6), 2207–2217.
544 doi:10.1111/1462-2920.14257
- 545 Hofman-Kamińska, E., Bocherens, H., Borowik, T., Drucker, D. G., & Kowalczyk, R.
546 (2018). Stable isotope signatures of large herbivore foraging habitats across Europe.
547 *PLOS ONE*, 13(1), e0190723. doi:10.1371/journal.pone.0190723
- 548 Hooper, L. V., Littman, D. R., & Macpherson, A. J. (2012). Interactions between the
549 microbiota and the immune system. *Science*, 336(6086), 1268–1273.
550 doi:10.1126/science.1223490
- 551 Hundertmark, K. J., Bowyer, R. T., Shields, G. F., & Schwartz, C. C. (2003). Mitochondrial
552 phylogeography of moose (*Alces alces*) in North America. *Journal of Mammalogy*,
553 84(2), 718–728. doi:10.1644/1545-1542(2003)084<0718:MPOMAA>2.0.CO;2
- 554 Ishaq, S. L., Sundset, M. A., Crouse, J., & Wright, A.-D. G. (2015). High-throughput DNA
555 sequencing of the moose rumen from different geographical locations reveals a core
556 ruminal methanogenic archaeal diversity and a differential ciliate protozoal diversity.
557 *Microbial Genomics*, 1(4), e000034. doi:10.1099/mgen.0.000034
- 558 Ishaq, S. L., & Wright, A.-D. G. (2012). Insight into the bacterial gut microbiome of the
559 North American moose (*Alces alces*). *BMC Microbiology*, 12(1), 212.
560 doi:10.1186/1471-2180-12-212
- 561 Ishaq, S. L., & Wright, A. D. (2014). High-throughput DNA sequencing of the ruminal
562 bacteria from moose (*Alces alces*) in Vermont, Alaska, and Norway. *Microbial Ecology*,
563 68(2), 185–195. doi:10.1007/s00248-014-0399-0

- 564 Jani, A. J., & Briggs, C. J. (2014). The pathogen *Batrachochytrium dendrobatidis* disturbs the
565 frog skin microbiome during a natural epidemic and experimental infection.
566 *Proceedings of the National Academy of Sciences*, *111*(47), E5049–E5058.
567 doi:10.1073/pnas.1412752111
- 568 Jani, A. J., & Briggs, C. J. (2018). Host and aquatic environment shape the amphibian skin
569 microbiome but effects on downstream resistance to the pathogen *Batrachochytrium*
570 *dendrobatidis* are variable. *Frontiers in Microbiology*, *9*(MAR), 487.
571 doi:10.3389/fmicb.2018.00487
- 572 Kammann, E. E., & Wand, M. P. (2003). Geoadditive models. *Journal of the Royal*
573 *Statistical Society: Series C (Applied Statistics)*, *52*(1), 1–18. doi:10.1111/1467-
574 9876.00385
- 575 Kanehisa, M., Sato, Y., Kawashima, M., Furumichi, M., & Tanabe, M. (2016). KEGG as a
576 reference resource for gene and protein annotation. *Nucleic Acids Research*, *44*(D1),
577 D457–D462. doi:10.1093/nar/gkv1070
- 578 Kohl, K. D., Varner, J., Wilkening, J. L., & Dearing, M. D. (2018). Gut microbial
579 communities of American pikas (*Ochotona princeps*): Evidence for phylosymbiosis
580 and adaptations to novel diets. *Journal of Animal Ecology*, *87*(2), 323–330.
581 doi:10.1111/1365-2656.12692
- 582 Langille, M. G. I., Zaneveld, J., Caporaso, J. G., McDonald, D., Knights, D., Reyes, J. A., ...
583 Huttenhower, C. (2013). Predictive functional profiling of microbial communities using
584 16S rRNA marker gene sequences. *Nature Biotechnology*, *31*(9), 814–821.
585 doi:10.1038/nbt.2676
- 586 Le Borgne, H., Hébert, C., Dupuch, A., Bichet, O., Pinaud, D., & Fortin, D. (2018). Temporal
587 dynamics in animal community assembly during post-logging succession in boreal
588 forest. *PLOS ONE*, *13*(9), e0204445. doi:10.1371/journal.pone.0204445

- 589 Lee, J. D., & Hastie, T. J. (2015). Learning the structure of mixed graphical models. *Journal*
590 *of Computational and Graphical Statistics*, 24(1), 230–253.
591 doi:10.1080/10618600.2014.900500
- 592 Lenarz, M. S. (2009). *2009 Aerial Moose Survey*. St Paul, USA.
- 593 Ley, R. E., Hamady, M., Lozupone, C., Turnbaugh, P. J., Ramey, R. R., Bircher, J. S., ...
594 Gordon, J. I. (2008). Evolution of mammals and their gut microbes. *Science*, 320(5883),
595 1647–1651. doi:10.1126/science.1155725
- 596 Masella, A. P., Bartram, A. K., Truszkowski, J. M., Brown, D. G., & Neufeld, J. D. (2012).
597 PANDAseq: paired-end assembler for illumina sequences. *BMC Bioinformatics*, 13(1),
598 31. doi:10.1186/1471-2105-13-31
- 599 McKenney, E. A., Williamson, L., Yoder, A. D., Rawls, J. F., Bilbo, S. D., & Parker, W.
600 (2015). Alteration of the rat cecal microbiome during colonization with the helminth
601 *Hymenolepis diminuta*. *Gut Microbes*, 6(3), 182–193.
602 doi:10.1080/19490976.2015.1047128
- 603 Methé, B. A., Nelson, K. E., Pop, M., Creasy, H. H., Giglio, M. G., Huttenhower, C., ...
604 White, O. (2012). A framework for human microbiome research. *Nature*, 486(7402),
605 215–221. doi:10.1038/nature11209
- 606 Moeller, A. H., Peeters, M., Ayoub, A., Ngole, E. M., Esteban, A., Hahn, B. H., & Ochman,
607 H. (2015). Stability of the gorilla microbiome despite simian immunodeficiency virus
608 infection. *Molecular Ecology*, 24(3), 690–697. doi:10.1111/mec.13057
- 609 Moeller, A. H., Suzuki, T. A., Lin, D., Lacey, E. A., Wasser, S. K., & Nachman, M. W.
610 (2017). Dispersal limitation promotes the diversification of the mammalian gut
611 microbiota. *Proceedings of the National Academy of Sciences of the United States of*
612 *America*, 114(52), 13768–13773. doi:10.1073/pnas.1700122114
- 613 Mshelia, E. S., Adamu, L., Wakil, Y., Turaki, U. A., Gulani, I. A., & Musa, J. (2018). The

- 614 association between gut microbiome, sex, age and body condition scores of horses in
615 Maiduguri and its environs. *Microbial Pathogenesis*, 118, 81–86.
616 doi:10.1016/j.micpath.2018.03.018
- 617 Muegge, B. D., Kuczynski, J., Knights, D., Clemente, J. C., González, A., Fontana, L., ...
618 Gordon, J. I. (2011). Diet drives convergence in gut microbiome functions across
619 mammalian phylogeny and within humans. *Science*, 332(6032), 970–4.
620 doi:10.1126/science.1198719
- 621 Murray, D. L., Cox, E. W., Ballard, W. B., Whitlaw, H. A., Lenarz, M. S., Custer, T. W., ...
622 Fuller, T. K. (2006). Pathogens, nutritional deficiency, and climate influences on a
623 declining moose population. *Wildlife Monographs*, 166(1), 1–30. doi:10.2193/0084-
624 0173(2006)166[1:PNDACI]2.0.CO;2
- 625 Näpflin, K., & Schmid-Hempel, P. (2018). Host effects on microbiota community assembly.
626 *Journal of Animal Ecology*, 87(2), 331–340. doi:10.1111/1365-2656.12768
- 627 Nemergut, D. R., Schmidt, S. K., Fukami, T., O’Neill, S. P., Bilinski, T. M., Stanish, L. F.,
628 ... Ferrenberg, S. (2013). Patterns and processes of microbial community assembly.
629 *Microbiology and Molecular Biology Reviews*: *MMBR*, 77(3), 342–56.
630 doi:10.1128/MMBR.00051-12
- 631 Oksanen, J., Blanchet, F. G., Kindt, R., Legendre, P., Minchin, P. R., O’Hara, R. B., ...
632 Wagner, H. (2013). Package ‘vegan.’ *R Package Ver. 2.0–8*, 254.
- 633 Ovaskainen, O., Abrego, N., Halme, P., & Dunson, D. (2016). Using latent variable models
634 to identify large networks of species-to-species associations at different spatial scales.
635 *Methods in Ecology and Evolution*, 7(5), 549–555. doi:10.1111/2041-210X.12501
- 636 Ovaskainen, O., Tikhonov, G., Norberg, A., Guillaume Blanchet, F., Duan, L., Dunson, D.,
637 ... Abrego, N. (2017). How to make more out of community data? A conceptual
638 framework and its implementation as models and software. *Ecology Letters*, 20(5), 561–

- 639 576. doi:10.1111/ele.12757
- 640 Severud, W. (2017). *Assessing calf survival and the quantitative impact of reproductive*
641 *success on the declining moose (Alces alces) population in northeastern Minnesota.*
642 University of Minnesota. Retrieved from
643 <https://conservancy.umn.edu/handle/11299/191446>
- 644 Svartström, O., Alneberg, J., Terrapon, N., Lombard, V., De Bruijn, I., Malmsten, J., ...
645 Andersson, A. F. (2017). Ninety-nine de novo assembled genomes from the moose
646 (*Alces alces*) rumen microbiome provide new insights into microbial plant biomass
647 degradation. *ISME Journal*, 11(11), 2538–2551. doi:10.1038/ismej.2017.108
- 648 Vellend, M., Srivastava, D. S., Anderson, K. M., Brown, C. D., Jankowski, J. E., Kleynhans,
649 E. J., ... Xue, X. (2014). Assessing the relative importance of neutral stochasticity in
650 ecological communities. *Oikos*, 123(12), 1420–1430. doi:10.1111/oik.01493
- 651 Wood, S. N. (2003). Thin plate regression splines. *Journal of the Royal Statistical Society:*
652 *Series B (Statistical Methodology)*, 65(1), 95–114. doi:10.1111/1467-9868.00374
- 653 Wünschmann, A., Armien, A. G., Butler, E., Schrage, M., Stromberg, B., Bender, J. B., ...
654 Carstensen, M. (2015). Necropsy findings in 62 opportunistically collected free-ranging
655 moose (*Alces alces*) from Minnesota, USA (2003–13). *Journal of Wildlife Diseases*,
656 51(1), 157–165. doi:10.7589/2014-02-037
- 657 Zelezniak, A., Andrejev, S., Ponomarova, O., Mende, D. R., Bork, P., & Patil, K. R. (2015).
658 Metabolic dependencies drive species co-occurrence in diverse microbial communities.
659 *Proceedings of the National Academy of Sciences of the United States of America*,
660 112(20), 6449–54. doi:10.1073/pnas.1421834112
- 661 Zhou, J., & Ning, D. (2017). Stochastic community assembly: Does it matter in Microbial
662 Ecology? *Microbiology and Molecular Biology Reviews* □: *MMBR*, 81(4), e00002-17.
663 doi:10.1128/MMBR.00002-17

